Springer

Journal of Mechanical Science and Technology 23 (2009) 1446~1455

Journal of Mechanical Science and Technology

www.springerlink.com/content/1738-494x
DOI 10.1007/s12206-009-0349-9

Passive acoustic radiation control for a vibrating panel with piezoelectric shunt damping circuit using particle swarm optimization algorithm †

Jin-Young Jeon*

Digital Printing Division, Digital Media & Communications Business, Samsung Electronics Co., Ltd., Suwon-City, 443-742, Korea

(Manuscript Received August 6, 2008; Revised March 2, 2009; Accepted March 6, 2009)

Abstract

This paper presents a new acoustic radiation optimization method for a vibrating panel-like structure with a passive piezoelectric shunt damping system in order to minimize well-radiating modes generated from the panel. The optimization method is based on an idea of using the p-version finite element method(p-version FEM), the boundary element method(BEM), and the particle swarm optimization algorithm(PSOA). Optimum embossment design for the vibrating panel using the PSOA is first investigated in order to minimize noise radiation over a frequency range of interest. The optimum embossment design works as a kind of stiffener so that well-radiating natural modes are shifted up with some degrees. The optimized panel, however, may still require additional damping for attenuating the peak acoustic amplitudes. A passive shunt damping system is thus employed to additionally damp the well-radiating modes from the optimized panel. To numerically evaluate the acoustic multiple-mode damping capability by a shunt damping system, the integrated p-version FEM/BEM for the panel with the shunt damping system is modeled and developed by MATLAB. Using the PSOA, the optimization technique for the optimal multiple-mode shunt damper is investigated in order to achieve the optimum damping performance for the well-radiating modes simultaneously. Also, the acoustic damping performance of the shunt damping circuit in the acoustic environment is demonstrated numerically and experimentally with respect to the realistically sized panel. The simulated result shows a good agreement with that of the experimental result.

Keywords: Shunt damping system; P-version FEM; BEM; Sound power level; Particle swarm optimization algorithm

1. Introduction

Design for desired sound emission characteristics, as well as design for the addition of vibration damping, are important and challenging problems. Significant progress has been made in the development and validation of numerical techniques for the accurate prediction of the acoustic emission of noise from vibration structures of general shape. However, in many structural design problems vibration and noise are difficult to control in the post-fabrication stage. This makes it necessary to take into account noise and vibration at an early design stage. With limited computational time-power capacities, it is important to know which parts of a structure have the strongest effect on the objective function. The possibility to accomplish this without the need to run extensive parametric studies would greatly facilitate design refinement and optimization. Then, acoustic radiation optimization has been studied to improve such products from the viewpoint[1].

There are some publications concerning acoustic radiation optimization as briefly reviewed below. Tinnsten et al.[2] presented a comparison of the numerical result and the experimental result for minimizing acoustic emission emanating from a cylinder having top and bottom shell plates by using simulated annealing(SA). The thickness in one boundary sur-

† This paper was recommended for publication in revised form by Associate Editor Yeon June Kang

*Corresponding author. Tel.: +82 31 200 4096, Fax.: +82 31 200 5016
E-mail address: jinyoungls.jeon@samsung.com

face of shell structure was employed as design variable. The results provided by Kaneda et al.[3] indicated the advantages and the validity of the optimized geometry of plate curvature for reducing sound power effectively. Micro genetic algorithm (MGA) was used to optimize plate geometry. These approaches, however, may still require the addition of passive or active damping for attenuating the shifted peak vibration amplitudes generated from the optimized structures.

The application of piezoelectric materials with different control configurations(such as active control, shunted control, etc.) for reducing vibration and structure-borne noise has been studied by many researchers in the past few years. Almost all of the studies have involved the implementation of an active control system for reducing acoustic radiation from a vibrating structure, also referred to as structure-borne noise. [4-6] Within active control systems, the piezoelectrics require complex amplifiers and associated sensing electronics. These can be eliminated in passive shunting applications where the only external element is a simple passive electrical circuit.

In recent years, the passive shunt damping systems employing the piezoelectric materials have been used to attenuate the peak vibration amplitudes from the vibrating structures. Piezoelectric materials can be used for producing the structural damping because of their unique ability to efficiently transform mechanical energy into electrical energy and vice versa, as shown in Fig. 1.

Piezoelectric shunts using a resistor and an inductor in series have been studied by Hagood and Flotow[7]. They presented an analytical model of the shunted piezoelectric with the experimental verification of the model using a resistive and a series resonant shunt to provide damping for the cantilevered beam. Davis and Lesieutre[8] developed a method for predicting the passive damping in beams with resistively shunted piezoelectric patches based on the strain energy dissipation approach, and reported experimental results.

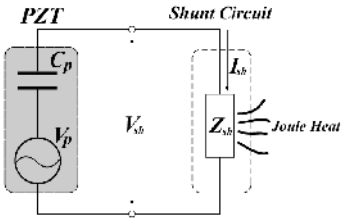

Fig. 1. Equivalent electrical model of a PZT.

Hollkamp[9] expanded the theory of piezoelectric shunting for a single mode so that a single piezoelectric material can be used to suppress two modes by optimally designing the shunting parameters. The multimode damper was demonstrated experimentally as a two-mode device applied to a cantilever beam. Wu et al.[10] described the principle of the multiple-mode shunting and the generalized shunt circuit employed to shunt-damp multiple modes simultaneously using only a single PZT. However, most of the above reported work on passive piezoelectric damping has been investigated in order to dampen the peak vibration amplitudes from a simple laminate or limited structural (mostly cantilevered beam) configurations. In modeling piezoelectric structures with shunt circuits, the conventional mechanical impedance model has been used.

Some researchers have studied passive shunt damping systems for reducing acoustic radiation of a vibrating structure. Kim et al.[11] presented a new tuning method for passive piezoelectric damping that is based on the electrical impedance model and maximum dissipated energy method. A panel-like structure mounted in a square cross-section tunnel was used as an example to verify the acoustic damping performance of the proposed method in realistically sized structures and multi-mode damping. Two piezoelectric wafers were used to take into account the edge and center modes of the plate individually and 7~10 dB reductions were experimentally achieved at these modes. Ahmadian et al.[12] investigated a detailed analysis of the experimental results of sound transmission tests for three different test plates, namely an undamped plate, a plate with constrained layer damping, and a plate with electrically shunted piezoceramic materials(PZTs). But they did not produce any theoretical result for an acoustic test.

Although the above-mentioned studies have provided valuable experimental results for acoustic damping performance with respect to the vibrating panel structures with several piezoelectric patches, a detailed analysis of the simulated result by acoustic radiation analysis seems to be required.

In this paper, author proposes a new acoustic radiation optimization method for a vibrating panel-like structure with passive piezoelectric shunt damping circuit in order to minimize several well-radiating modes generated from the panel. The optimization method is based on an idea of using the p-version finite element method(p-version FEM), the boundary

element method(BEM), and the particle swarm optimization algorithm(PSOA). The purpose of the present study is to investigate the validity of the proposed optimization method for the optimum design of an embossed panel section in the panel and the optimum components of the piezoelectric shunt damping circuit to efficiently minimize well-radiating modes. The effectiveness of the optimum design method is demonstrated by basic applications in simulation and experiment using an aluminum panel under a point force excitation in the frequency range from 50 [Hz] to 500 [Hz]. To numerically evaluate the acoustic damping performance with respect to the optimized panel with a piezoelectric shunt damper, the coupled p-version FEM/BEM model is modeled and developed by using MATLAB. The optimization technique for a piezoelectric shunt damper based on the PSOA is proposed to optimally tune the shunt electrical components for wholly minimizing the amplitude of an average velocity transfer function over a frequency range of interest.

2. Structural-acoustic analysis for the global system with the piezoelectric damper

In the present study, an acoustic radiation optimization of a clamped panel is performed in order to minimize noise radiation. The technical theory for the acoustic optimization is described in this section. A passive shunting control system is employed to additionally damp multiple-mode well-radiating modes from the optimum embossed panel in Fig. 9, which was obtained by acoustic radiation optimization based on the PSOA. The passive piezoelectric damper is an energy dissipation mechanism. The electrical impedance in the passive control system, as described in Fig. 1, is connected to the piezoelectric electrodes to dissipate electrical energy into the shunt damping circuit in the form of joule heating energy. The electromechanical coupling analysis of the global system with the shunted piezoelectric is described in this section. A three-dimensional finite element code using the p-version FEM is developed in order to analyze the electromechanical model of piezoelectric materials using MATLAB. Also, the boundary element method (BEM) is demonstrated analytically to evaluate the resultant reduction effect of acoustic radiation obtained by using the piezoelectric shunt damping system. The outline of the implementation of PSOA in the acoustic optimization computation is described.

2.1 Electro-structural analysis using p-version FEM

The fundamental property of piezoelectric materials is their ability to generate charge from an applied stress and conversely to generate stress from an applied electrical field. After the application of Hamilton's principle and finite element discretization for coupled electromechanical systems, the coupled finite element matrix equations for each element model can be derived in terms of extended nodal displacements as:

$$\begin{bmatrix} M & 0 \\ 0 & 0 \end{bmatrix}\begin{Bmatrix} \ddot{w} \\ \ddot{v} \end{Bmatrix}+\begin{bmatrix} C & 0 \\ 0 & 0 \end{bmatrix}\begin{Bmatrix} \dot{w} \\ \dot{v} \end{Bmatrix}+\begin{bmatrix} K & \Theta \\ \Theta^t & -C_P \end{bmatrix}\begin{Bmatrix} w \\ v \end{Bmatrix}=\begin{Bmatrix} F \\ q \end{Bmatrix} \quad (1)$$

where $[M]$, $[C]$, $[K]$ and $[\Theta]$ represent the global mass matrix, the global damping matrix, the global stiffness matrix and the electromechanical coupling matrix of the host structure and the piezoelectric material, respectively, $[C_P]$ is the inherent piezoelectric capacitance matrix, $\{F\}$ is the applied mechanical force vector, $\{q\}$ is the electric charge vector, $\{w\}$ is the generalized mechanical coordinate and $\{v\}$ is the generalized electrical coordinate, which is the physical voltage at the piezoelectric electrodes. The damping matrix $[C]$ is assumed to be a proportional viscous damping, which represents internal structural damping[13]. In the present study, p-version FEM using an eight-node, 32 degree-of-freedom brick element together with the shape functions of incompatible modes is developed for the piezoelectric analysis of a clamped panel with the bonded piezoelectric material, as depicted in Fig. 9. When a piezoelectric patch is shunted by an impedance Z_{sh}, the shunt damping voltage across the shunt damping network can be represented by the current-voltage relationship in the Laplace domain as:

$$V_{sh}(s) = Z_{sh}(s) \cdot I_{sh}(s) \quad (2)$$

where $V_{sh}(s)$ is the voltage across the impedance and $I_{sh}(s)$ is the current flowing through the impedance.

The governing equation of the shunted piezoelectric can be derived by considering the additional passive piezoelectric damping force as follows:

$$[M]\{\ddot{w}\}+\left([C]+Z_{total}[\Theta][\Theta]^t\right)\{\dot{w}\} +[K]\{w\}=\{F\} \quad (3)$$

where the total electrical impedance of the shunted piezoelectric Z_{total} includes the inherent capacitance of the piezoelectric and can be expressed by

$$Z_{total} = \frac{Z_{sh}}{1 + Z_{sh} C_p s}. \tag{4}$$

The velocity transfer function for a structure with the shunted piezoelectric can be expressed in the modal coordinates as follows:

$$D(\omega) = \frac{\dot{W}_j(\omega)}{F_i} = \sum_{r=1}^{N} \frac{\phi_{ri} \cdot \phi_{rj}}{m_r j\omega + (c_r + Z_{total} \cdot \theta_r) + k_r/(j\omega)} \tag{5}$$

where ϕ_{ri} and ϕ_{rj} are the elements i and j, respectively, of the r th eigenvector matrix.

2.2 Acoustic radiation analysis using BEM

In this section, the direct boundary element method (BEM) developed by MATLAB is briefly reviewed, because acoustic analysis is performed to theoretically predict the shunt damping capability of a vibrating panel with the bonded piezoelectric material.

The direct BEM solves the Helmholtz equation with respect to an unbounded exterior domain at a time. The primary variable in the boundary integral equation is sound pressure. Then, with respect to an acoustic field as shown in Fig. 2, the Helmholtz integral equation can be written in the formal way as follows:

$$p(P) = -\int_S \left[j\rho\omega \tilde{v}_n(Q) \Psi(Q,P) + p(Q) \frac{\partial \Psi}{\partial n}(Q,P) \right] dS(Q) \tag{6}$$

where p is sound pressure, Q and P are the field and source points, respectively, and ρ is air density. Ψ is the fundamental solution (called Green's function) in a three-dimensional free space which is expressed as:

$$\Psi(Q,P) = \frac{1}{4\pi R} e^{-jkR} \tag{7}$$

where $k = \omega/c'$ is the wave number, c' is the sound speed in air, and R is the distance of arbitrary points in Q from P. Note that the normal unit vectors n on the boundary surface S, which is discretized into boundary elements, are pointed into the negative normal direction. Equation (6) shows that the sound pressure $p(P)$, at arbitrary point P, inside the acoustic domain, Ω, can be obtained by integrating the equation on the boundary.

Applying a boundary element discretization procedure to Eq.(6), the linear system of equations is expressed as:

$$H(\omega)\, p(\omega) = G(\omega) \tilde{v}_n(\omega) \tag{8}$$

where $H(\omega)$ and $G(\omega)$ are the global complex frequency dependent system matrices. The four-node quadrilateral elements are used for the discretization of the specimen structure.

The total radiated sound power can be obtained by spatial integration of the mean square sound pressures at 13 observation points over the virtual hemispherical surface (see Fig. 3). In discretized form for numerical computation, the total radiation sound power level W can be expressed as:

$$W_o = \frac{2\pi r^2}{\rho c} \sum_{i=1}^{m} \frac{p_i^2}{m} \tag{9a}$$

$$W = 10 \log_{10}(W_o / W_{ref}) \text{ [dB]} \tag{9b}$$

where W_{ref} is the reference sound power, equal to 10^{-12} [W], p_i is the mean square sound pressure at the i th observation point, $2\pi r^2$ is the surface area of the hemisphere with radius r, and m is the number of the observation point.

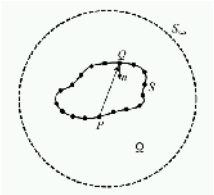

Fig. 2. Exterior problem.

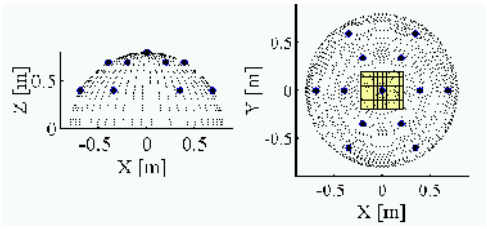

Fig. 3. Observation points.

2.3 Particle Swarm Optimization

The particle swarm optimization (PSO), which was proposed by Kennedy and Eberhart[14], originated from a simulation algorithm for simplified social behavior of organisms, such as bird flocking and fish schooling, developed by zoologists. It comprises a very simple concept that requires only primitive mathematical operators so that it is computationally inexpensive in terms of both computer memory and speed.

Let q be the number of the PSO population. For particle d ($d = 1,2,.....q$), Kennedy and Eberhart initially proposed that, for simulating the social behavior of birds, the position x^d in PSO be updated as:

$$x_{k+1}^d = x_k^d + v_{k+1}^d \tag{10}$$

and the velocity v^d be updated as:

$$v_{k+1}^d = v_k^d + c_1 r_1 (p_k^d - x_k^d) + c_2 r_2 (p_k^g - x_k^d) \tag{11}$$

where the subscript k is a time increment counter, r_1 and r_2 are stochastic factors in the range [0,1] , c_1 and c_2 are constants, called acceleration coefficients, that are recommended by the developers and that control the maximum step size the particle can perform, p_k^d represents the best ever position (i.e., the best position of the d th particle that minimizes the objective function until the k th optimization process) of particle d at time k , and p_k^g represents the global best ever position (i.e., the global best position among all particles that minimizes the objective function until the k th optimization process) in the swarm until time k .

Furthermore, by adding a new inertia weight λ into Eq. (11), a new modified formulation of PSO was proposed by Eberhart et al.[15] as follows:

$$v_{k+1}^d = \lambda v_k^d + c_1 r_1 (p_k^d - x_k^d) + c_2 r_2 (p_k^g - x_k^d) \tag{12}$$

They proposed $0.8 < \lambda < 1.4$ as the appropriate range of λ . The inertia weight, which is a user-specified parameter, is used to control the impact of the previous historical values of the particle velocities on the current velocity. A larger inertia weight facilitates flying toward global exploration, searching a new area, while a smaller inertia weight tends to facilitate fine-tuning of the current search area. Appropriate selection of the inertia weight and acceleration coefficients can provide a balance between global and local exploration abilities, and thus, on average, the optimal solution can be found in fewer iterations. Equation (11) is employed in order to obtain the new velocity of the particle according to its previous velocity and the distance of its current position from both its own best historical position and its neighbors' best position. Then, the particle d in PSO moves to a new position according to Eq. (10).

2.4 PSO algorithm for acoustic radiation optimization

This section describes the implementation of PSOA for the acoustic optimization method. The main purpose of the acoustic optimization method is to minimize the sound power radiated from a panel-like structure or component in machines. Then, the average radiated sound power A_w over a frequency range of interest, which is derived from the total radiated sound power W in Eq. (9), is adopted as the objective function to be minimized in the second process. In tuning the optimal parameter for the piezoelectric shunt damping circuit, the average velocity transfer function B_w over a frequency range of interest, which is derived from the velocity transfer function D in Eq. (5), is adopted as the objective function to be minimized in the third process. The average radiated sound power, average velocity transfer function and the objective function are expressed by Eqs (13a) and (13b), respectively.

$$A_w = \frac{1}{N_f} \sum_{i=1}^{N_f} W(\omega_i), \quad B_w = \frac{1}{N_f} \sum_{i=1}^{N_f} D(\omega_i) \tag{13a}$$

$$\text{Minimize } A_w,\ B_w \tag{13b}$$

The feasible design area of the variables must be bounded in practice. Then, the upper and lower bounds of the design variables are expressed as:

$$\underline{x}(i) \le x(i) \le \overline{x}(i) \quad (i = 1 \sim 3) \tag{14}$$

where $\underline{x}(i)$ and $\overline{x}(i)$ are the lower and the upper boundary of design variable number i , respectively.

3. Acoustic radiation optimization for a clamped panel

3.1 Numerical and experimental configurations

As a basic application to verify the acoustic optimization method, an aluminum panel under clamping its four edge lines is dealt with under a point exciting force having the amplitude of 1 N in the frequency range of 50~500Hz. It has the dimensions of $0.45\times0.4\,\mathrm{m}$ with thickness $0.001\,\mathrm{m}$. The material properties of the aluminum panel (JIS A5052) are Young's modulus of 69.3 GPa, Poisson's ratio of 0.33, and density of $2680\,\mathrm{kg/m^3}$. The panel is assumed to be in an infinite baffle. The panel is under applying a point exciting force at the center, whose coordinate is (0.0,0.0,0.0), of the panel. The application is performed with respect to the frequency range of 50~500 [Hz]. The computational frequency interval is 1 [Hz]. The acoustic medium is air having a density of $1.21\mathrm{kg/m^3}$ and sound speed of $343\,\mathrm{m/s}$. In the acoustic optimization process, observation points are symmetrically employed at 13 points on the hemispherical surface $0.8m$ away from the center of the panel.

To confirm the validity of the above-mentioned simulation method, an experiment is carried out. Fig. 4 illustrates actual panel clamped on a box-like test bench that can be assumed to be rigid. Raised sections are made in the experimental panels by embossing wisely by a professional industrial technician using a press machine.

The experiments are carried out using a sound intensity measurement system in a semi-anechoic chamber. The sound power level(SPL) is obtained in accordance with sound intensity measurement at discrete points (ISO 9614-1:1993), which is related to the imaginary part of the cross spectrum between two microphones.

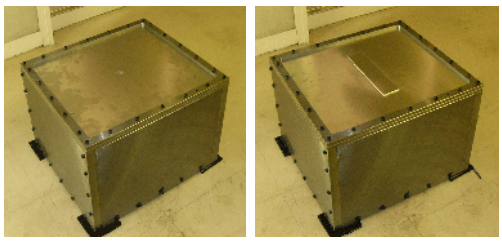

(a) Original panel (b) Optimized panel

Fig. 4. Clamped panel.

3.2 Acoustic radiation optimization using PSOA

The implementation of the acoustic optimization problem under excitation at the center point of the panel is presented in this section. As expressed in the dotted line in Fig. 5, the integrated p-version FEM/BEM analysis computes the radiated sound power of the original flat panel having six well-radiating natural modes at 49.9, 165.1, 199.7, 302.4, 380.8, and 473.6 [Hz], respectively. The radiated sound power from the panel with the optimum embossed panel section is computationally predicted as shown in solid line in Fig. 5.

The optimum embossed panel section works as a kind of stiffener so that well-radiating natural modes are shifted up to some degree. Fig. 6 indicates that the proposed acoustic radiation optimization will be able to give us a good design of the embossed panel section that can decrease the SPL from 102.3 dB to 88.8 dB over the given frequency, 50~500 [Hz] in 1 [Hz] steps. That is, a reduction of about 14 dB. Fig. 6 shows that a big reduction of the objective function is achieved after about ten iterations and that the solution converged after about 80 iterations. The program was made by the author using MATLAB. It took about 1 hour for one iteration using a personal computer with Pentium 4 having 2.4 GHz and 1GB RAM.

The resultant embossed panel section has the dimensions of height ($0.004\,\mathrm{m}$), width ($0.054\,\mathrm{m}$), and length ($0.237\,\mathrm{m}$).

Fig. 7 shows the sound powers obtained by experiment. The dotted line represents the SPL radiated from the original panel shown in Fig. 4(a) under a point force excitation having the amplitude of 1 N in the frequency range of interest. The solid line presents the SPL of the optimized panel shown in Fig. 4(b).

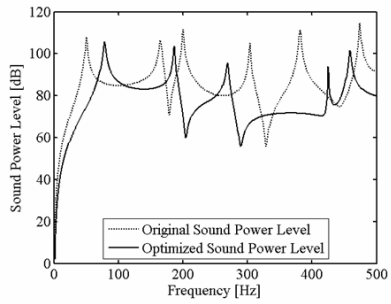

Fig. 5. Comparison of the SPL for original and optimized panel in excitation at center point.

The result of the experiment ensures that noise reduction of the panel is successfully achieved over the given frequency range. Precisely comparing the experimental result in Fig. 7 to the simulation result in Fig. 5, it is found that the natural frequencies of the experimental result are slightly higher than those of the simulation results.

However, it can be admitted that the experimental result is in good agreement with the simulation and that the average sound power level was decreased from 102 dB to 88 dB over the given frequency range. That is, it is experimentally confirmed that the optimized panel can possibly achieve about 14 dB noise reduction of the average SPL. Furthermore, the sound pressure at a point (0.0,0.0,0.1) in time domain is measured, and is shown in Fig. 8. The impulse sound pressure response in time domain can make it clear that the optimized panel generates less noise than the original panel. However, there are still the shifted peak vibration amplitudes from the optimized panel over the frequency range of interest. The optimized panel may still require additional damping for attenuating the peak acoustic amplitudes.

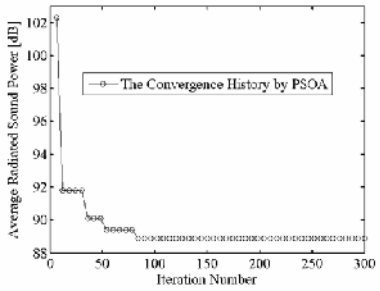

Fig. 6. The convergence history.

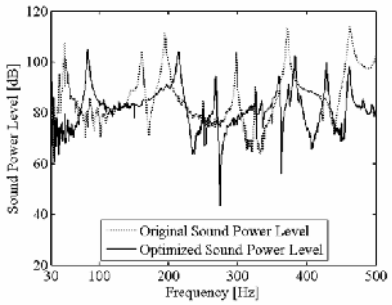

Fig. 7. Comparison of the SPL for original and optimized panel in excitation at center point.

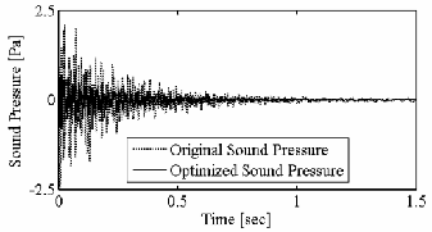

Fig. 8. Sound pressure time response.

4. Passive acoustic radiation control using piezoelectric shunt damping circuit

4.1 Numerical and experimental configurations

In this section, to confirm the validity of the simulation result, a piezoelectric damping experiment was performed in a semi-anechoic chamber. The shunt circuit chosen for this application is a modified series-parallel shunt circuit, similar to the one demonstrated by Wu. Although other shunting concepts exist, this shunt circuit was chosen because it had successfully been used for other applications[10]. Using the shunt damping circuit, the multiple-mode shunt damping experiment was performed to additionally damp the first and fourth well-radiating modes from the optimum panel, which was designed from the acoustic optimization computation. The acoustic optimum panel with a clamped boundary condition was performed to verify the acoustic damping effectiveness of the piezoelectric shunt circuit in this section. The PZT C-82 piezoelectric patch was bonded on the upper surface of the optimum embossed the panel by using a very thin layer of epoxy, as shown in Fig. 9. The location of the PZT was selected based on the p-version FEM/BEM and modal analysis testing. It has a size of 0.2×0.03 m with a thickness of 0.001m. The multiple-mode shunt damping circuit was wired in parallel to the electrodes of the PZT piezoelectric patch so that the shunted piezoelectric could damp several well-radiating modes of the panel with the

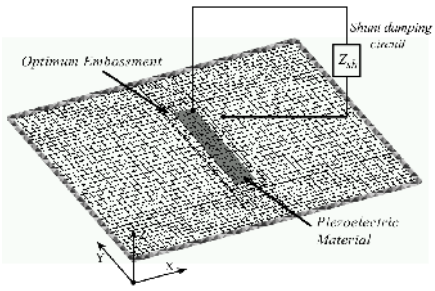

Fig. 9. A clamped panel with the shunted piezoelectric.

Table 1. Component values of the simplified circuit for the panel.

Circuit Components	Experimental Values	Simulated Values
C_1	1 μF	1 μF
C_2	1 μF	1 μF
L_1	3.21 H	3.21 H
L_2	0.50 H	0.49 H
R_1	23.1 kΩ	25.1 kΩ
R_2	30.1 kΩ	31.7 kΩ

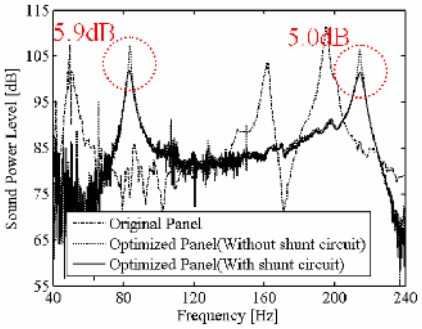

(a) Experimental frequency response

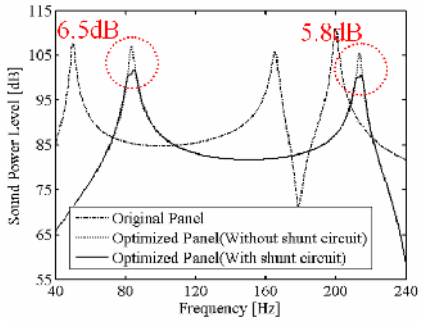

(b) Simulated frequency response

Fig. 10. Acoustic frequency responses of a realistic sized panel.

optimum embossment. Using a single PZT piezoelectric patch only, piezoelectric damping was implemented at two resonance modes simultaneously.

To search for the optimal shunt resistance R_i, the author employed an optimization technique based on the PSOA. The optimization technique was performed to search for the optimal parameter for wholly minimizing the amplitude of the average velocity transfer function over the frequency band of interest. Note that the capacitance ($C_p^T = 134$ nF) of the PZT piezoelectric at constant stress was measured by the impedance analyzer.

The acoustic experiments were done by using a sound intensity measurement system in a semi-anechoic chamber.

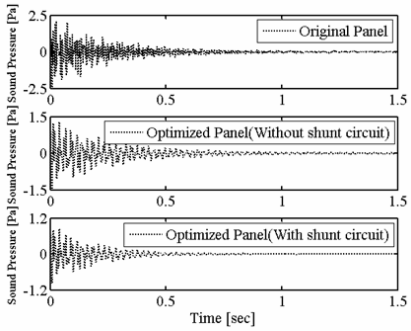

Fig. 11. Experimental time domain responses.

4.2 Multiple well-radiating modes damping

The Piezoelectric damping experiment was carried out to additionally dampen the first and fourth well-radiating modes of the vibrating panel with the optimum embossment. The experimental result, whose SPL is shown in Fig. 10(a), was measured to verify the acoustic damping performance with respect to the panel. A summary of the circuit components applied in the modified series-parallel shunt circuit is listed in Table 1. As shown in Fig. 10(a), the peak amplitudes at the first and fourth well-radiating modes were experimentally reduced by 5.9 dB and 5.0 dB, respectively. The simulation result shown in Fig. 10(b) was calculated by using the integrated p-version FEM/BEM method described in section 2. The peak amplitudes of the first and fourth modes were theoretically observed with reductions of 6.5 dB and 5.8 dB, respectively. The simulated result is in good agreement with the experimental result. The damping performance of the shunted piezoelectric can be further observed by comparing the SPL of the original panel, as shown by dashed line in Fig. 10.

Furthermore, the sound pressure at a point (0.0,0.0,0.1) in time domain was measured, and shown in Fig. 11. The impulse sound pressure responses in time domain show clearly that the shunted piezoelectric can sufficiently conduct the damping performance in the acoustic environment.

5. Conclusions

A new acoustic radiation optimization method has been proposed for a vibrating thin panel structure with passive piezoelectric shunt damping system in order to simultaneously damp several well-radiating modes from the panel. The optimization method is based on the integrated p-version FEM/BEM and the

particle swarm optimization algorithm(PSOA). The main purpose of the optimization method was to search for the optimum design of an embossed panel section in the panel and the optimum components of the piezoelectric shunt damping system in order to efficiently reduce noise. The validity of the optimum design method was demonstrated by basic applications in simulation and experiment using an aluminum panel under a point force excitation in the frequency range from 50 [Hz] to 500 [Hz].

Furthermore, to numerically predict the acoustic damping performance with respect to the optimized panel with a piezoelectric shunt damper, the coupled p-version FEM/BEM model was modeled and developed by using MATLAB. The optimization technique for a piezoelectric shunt damper based on the PSOA was proposed to optimally tune the shunt electrical components of the modified series-parallel shunt damping circuit.

In addition, to confirm the validity and effectiveness of the simulation result, a multiple-mode shunt damping experiment was done by using a sound intensity measurement system in a semi-anechoic chamber. The experiment was performed to verify the acoustic damping performance of the shunt circuit with respect to the optimized panel, which was theoretically demonstrated by the simulation. The piezoelectric damping experiment was carried out to additionally damp and reduce the 1st and 4th well-radiating modes generated from the optimized panel simultaneously.

Also, the impulse sound pressure sound responses in time domain obtained experimentally show clearly that the shunted piezoelectric patch can successfully damp the well-radiating modes of the clamped panel. The experimental result shows good agreement with the simulated result.

References

[1] S. T. Christensen, S. V. Sorokin and N. Olhoff, On analysis and optimization in structural acoustics-part I, *Structural Optimization*, 16, (1998) 83-95.

[2] M. Tinnsten, P. Carlsson and M. Jonsson, Stochastic optimization of acoustic response - a numerical and experimental comparison, *Struct Multidisc Optim*. 23, (2002) 405-411.

[3] S. Kaneda, Q. Yu, M. Shiratori and K. Motoyama, Optimization approach for reducing sound power from a vibration plate by its curvature design, *JSME Int. J. Series C*, 45(1), (2002) 87-98.

[4] M. Ruzzene and A. Baz, Active/passive control of sound radiation and power flow in fluid-loaded shells, *Journal of Thin-Walled Structures*, 38, (2000) 17-42.

[5] M. A. Simpson, T. M. Luong, C. R. Fuller and J. D. Jones, Full scale demonstration tests of cabin noise reduction using active vibration control, *Journal of Aircraft*, 30(3), (1992) 624-630.

[6] B. T. Wang, E. K. Dimitriadis and C. R. Fuller, Active control of structurally radiated noise using multiple piezoelectric actuators, *AIAA Journal*, 29(11), (1990) 1802-1809.

[7] N. W. Hagood and A. H. Von Flotow, Damping of structural vibrations with piezoelectric materials and passive electrical networks, *Journal of Sound and Vibration*, 146, (1991) 243-268.

[8] C. L. Davis and G. A. Lesieutre, A modal strain-energy approach to the prediction of resistively shunted piezoceramic damping, *Journal of Sound and Vibration*, 184, (1995) 489-513.

[9] J. J. Hollkamp, Multimodal passive vibration suppression with piezoelectric materials and resonant shunts, *J. Intell. Mater. Syst. Struct.*, 5, (1994) 49-57.

[10] S. Y. Wu, Method for multiple mode shunt damping of structural vibration using a single PZT transducer. *Proc. SPIE Smart Structures and Materials, Smart Structures and Intelligent Systems, SPIE* 3327, (1998) 159-168.

[11] J. H. Kim, Y. H. Ryu and S. B. Choi, New shunting parameter tuning method for piezoelectric damping based on measured electrical impedance, *Smart Mater. Struct.*, 9, (2000) 868-877.

[12] M. Ahmadian and K. M. Jeric, On the application of shunted piezoceramics for increasing acoustic transmission loss in structures, *Journal of Sound and Vibration*, 243(2), (2001) 347-359.

[13] D. F. Ostergaard and T. P. Pawlak, Three-dimensional finite elements for analyzing piezoelectric structures, *Proceedings of IEEE Ultrason. Symp.*, (1986) 639-644.

[14] J. Kennedy and R. Eberhart, Particle swarm optimization, *Proc. IEEE Int. Conf. On Neural Networks*, (1996) 1942-1948.

[15] R. Eberhart and Y. Shi, Comparison between genetic algorithms and particle swarm optimization, *7-th Annual Conf. On Evolutionary Programming*, (1998) 611-616.

Jin-Young Jeon received his Ph.D. degree in Mechanical and Aerospace Engineering from Tokyo Institute of Technology in 2005. Dr. Jeon is currently a senior engineer at Digital Printing Division, Digital Media & Communications Business at Samsung Elec-tronics Co., Ltd., Korea. His research interests are the areas of structural-acoustic optimization, sound quality, motion quality, and vibration control.